Available online at www.sciencedirect.com
SCIENCE DIRECT®
European Polymer Journal 40 (2004) 1987–1995
EUROPEAN POLYMER JOURNAL
www.elsevier.com/locate/europolj

Space charge distribution and crystalline structure in polyethylene blended with EVOH

Weichuan Du, Wei Zhong, Yijian Lin, Liang Shen, Qiangguo Du *

The Key Laboratory of Molecular Engineering of Polymer, Department of Macromolecular Science, Fudan University, Handan Road 220, Shanghai 200433, China

Received 2 May 2003; received in revised form 15 March 2004; accepted 7 April 2004
Available online 9 June 2004

Abstract

The space charge distribution in polyethylene samples under direct current (DC) electrical field was measured by pulsed electro-acoustic (PEA) method. It was found that by blending with 5 wt.% of poly(ethylene-co-vinyl alcohol) (EVOH) in low-density polyethylene (LDPE) the amount of accumulated space charges decreased and the field distribution of space charge improved. The differential scanning calorimetry (DSC) study showed that crystallization of LDPE/EVOH started at a higher temperature than LDPE. The results of wide-angle X-ray diffraction (WAXD) and small-angle light scattering (SALS) for LDPE/EVOH indicated that the crystal forms did not change, whereas the spherulites became smaller and imperfective. It can be seen from the results that EVOH played a role of nucleation during the crystallization of LDPE in the blend. The observation of scanning electron microscope (SEM) showed that the domains of EVOH were dispersed in LDPE as particles in diameter of 1 μm. The reduction of space charges in the blend sample can be explained as the results of the trapping of homo-charges at the interface and the dissipation of charges through LDPE matrix consisting of smaller spherulites.
© 2004 Elsevier Ltd. All rights reserved.

Keywords: Space charge distribution; Polyethylene; Poly(ethylene-co-vinyl alcohol); Nucleation; Crystallization; Interface

1. Introduction

Polymers and polymer blends are frequently used as insulators in electrical engineering and industry. In the case of DC voltage application, the accumulation of space charge can distort the electric field distribution in the polymer insulation matrix. Electric breakdown usually is caused by this uneven electric field distribution. It is, therefore, important to understand the mechanism of the formation and accumulation of space charges in power cable and to explore the means of elimination.

Polyethylene, due to its excellent electrical and mechanical properties, is widely used as insulation material for electric power cables. Numerous studies have been performed to investigate the space charge distribution and electrical conduction in polyethylene systems [1–4]. It was reported, for example, that the impulse breakdown strength of polyethylene can be improved by blending with ionomers [2] or ethylene-vinyl acetate copolymer [4]. The grafting technique has also been employed successfully to improve the electrical properties of polyethylene [5]. The PEA method was frequently used to measure the distribution of space charge accumulated under high DC field in cross-linked polyethylene [6] and in LDPE [7].

Polyethylene is a semi-crystalline polymer. It is conceivable that in a high DC field the crystalline structure is affected by the applied voltage, which in turn alters the distribution of space charges. Meunier and Crine

* Corresponding author. Tel.: +86-216-564-3891; fax: +86-216-564-0293.
E-mail address: qgdu@fudan.edu.cn (Q. Du).

0014-3057/$ - see front matter © 2004 Elsevier Ltd. All rights reserved.
doi:10.1016/j.eurpolymj.2004.04.003

reported a few years ago that polyethylene morphology was indeed modified when subjected to high fields and confirmed that the formation of tiny defects and microscopic cavities using infrared spectroscopy measurement (IR) [8,9]. There are also a few studies devoted to the relationship between charge distribution and crystalline morphology [10,11]. In our previous paper [12] we reported our finding that the space charge distribution in LDPE tended to be uniform by adding 0.3 wt.% of sorbitol as a nucleation agent and discussed the influence of crystallization microstructure on space charge.

In blends of semi-crystalline polymers, for the matter of crystalline morphology, it becomes much more complicated. Blending not only changes the morphologies of individual semi-crystalline polymers but also creates interfaces between different phases of the two polymers. In semi-crystalline polymers the interfaces between the amorphous and crystalline phases are well known trapping sites [13]. It is also possible that the trapping of charge occurs at the interfaces between the polymer phases. At present the understanding on the origins and distribution of space charge in the semi-crystalline polymer blends is still very limited. The complexity of morphology of semi-crystalline polymer blends renders much more studies. In this work 5 wt.% of EVOH was added to LDPE. The relationship between the distribution of space charge in the DC field and the morphology was investigated with PEA measurement, small-angle light scattering (SALS) test, scanning electron microscope (SEM) observation and differential scanning calorimetry (DSC) analysis.

2. Experimental

2.1. Materials

LDPE was cable grade product DJ200 (Melting Index of 2.1 g/10 min) of Shanghai Petrochemical Co. Ltd. EVOH containing 47 mol% ethylene (G156) was kindly provided by Kuraray Co. Ltd., Japan. The properties of the EVOH are listed in Table 1.

Table 1
Properties of EVOH used in this study

Ethylene content	47 (mol%)
Density	1.12 (g/cm)
T_m	160 (°C)
T_g	48 (°C)
M_n	15,400
M_w	48,200

2.2. Preparation of samples

EVOH was dried at 90 °C for 24 h in a vacuum oven. LDPE and 5 wt.% of EVOH were mixed in a Brabender Plasticorder with rotor speed of 40 rpm at the temperature of 195 °C for 5 min. The virgin LDPE was subjected to the same process to be used as a reference. Films of different thickness were prepared using a hot press at 170 °C for different length of time. Films of ~0.5 mm in thickness were for PEA and DSC experiments. Films of ~0.1 mm in thickness were for the SALS and WAXD studies.

2.3. Space charge measurement

The space charge distribution in samples was measured using pulsed electro-acoustic method as shown in Fig. 1 (DC source, 0–20 kV; pulse width, 20 ns; pulse voltage, 0–1 kV). The diameter of copper electrode was 25 mm. Aluminum was deposited on two sides of plate samples as electrodes. Silicone oil was used as an acoustic coupling agent in order to make a good acoustic contact between the sample electrode and the measuring electrode. The principle of this method and details of measurement were described in the previous paper [12].

2.4. DSC analysis

The Avrami exponent of crystallization was determined under non-isothermal conditions [14–17]. A Perkin Elmer DSC-7 was used for data acquisition and the thermal analysis. The sample was first rapidly heated up to 170 °C, approximately 60 °C higher than the melting point of LDPE, and then maintained at this temperature for 5 min in order to erase any previous morphological history that the sample might be carrying. The sample then non-isothermally crystallized under nitrogen when it was cooled down to 0 °C at selected cooling rates. The enthalpy of crystallization of 100% crystalline LDPE was taken from literature as 68.2 cal/g [18], and crystallinity of the sample was calculated from the crystallization enthalpy.

2.5. Depolarization measurement

The crystallization speed of the samples was measured using depolarization method on a GIY-III optical depolarization instrument at 85, 75 and 65 °C, respectively.

2.6. SALS

The Hv light scattering patterns were recorded on a small-angle light scattering photometer [19] equipped with a polarizer, an analyzer and a He–Ne laser source.

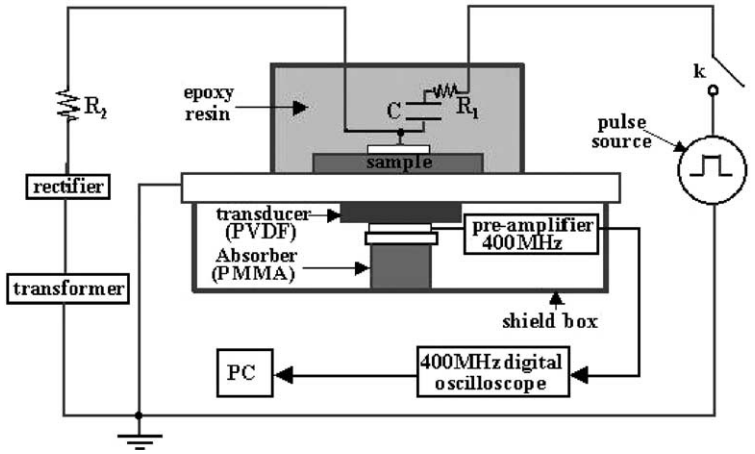

Fig. 1. Schematic diagram of apparatus for measurement of sample space charge distribution.

2.7. WAXD

WAXD measurements were carried out at room temperature on a D/max-rB diffractometer (Rigaku, Japan) equipped with a CuKα tube and Ni filter over a range of diffraction angle $2\theta = 5$–$50°$.

2.8. SEM observation

The morphology of the LDPE/EVOH blend sample, which was cryogenically fractured in liquid nitrogen and etched with nitric acid for 7 h, was observed with a JSM-5600LV scanning electron microscope (JEOL Corporation, Japan).

3. Results and discussion

3.1. Space charge distribution in samples

The PEA measurement gives a curve of space charge density (ρ) versus the vertical distance (*depth*) from the anode. Charge distributions in LDPE and LDPE/EVOH are shown in Figs. 2 and 3. The distance between the two vertical dotted lines is the depth of samples equal to the distance from anode to cathode, and the amount of space charges accumulated can be obtained from the absolute value of integral areas. Fig. 2 shows the charge distribution obtained while DC voltages were being applied at the stress of 10, 20, and 30 kV/mm. Fig. 3 presents the charge distribution after short circuit

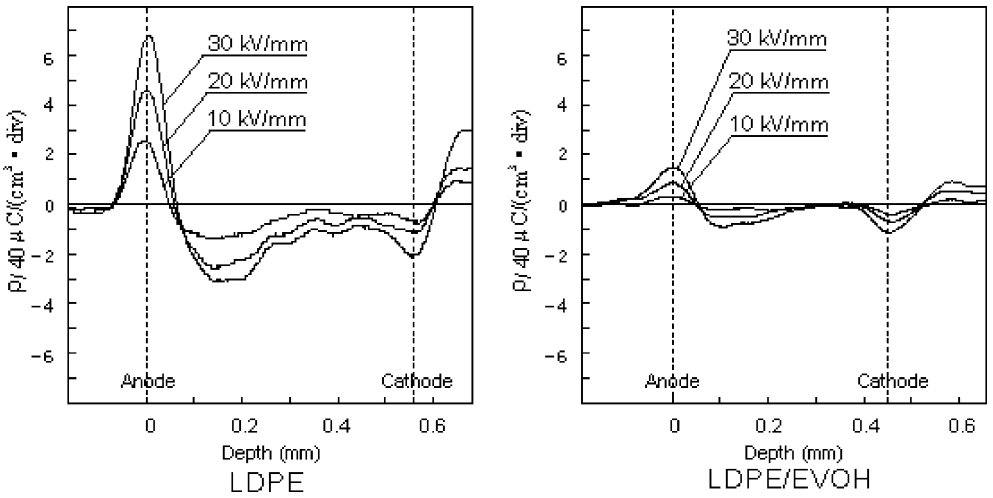

Fig. 2. Space charge distribution at various voltages of LDPE and LDPE/EVOH.

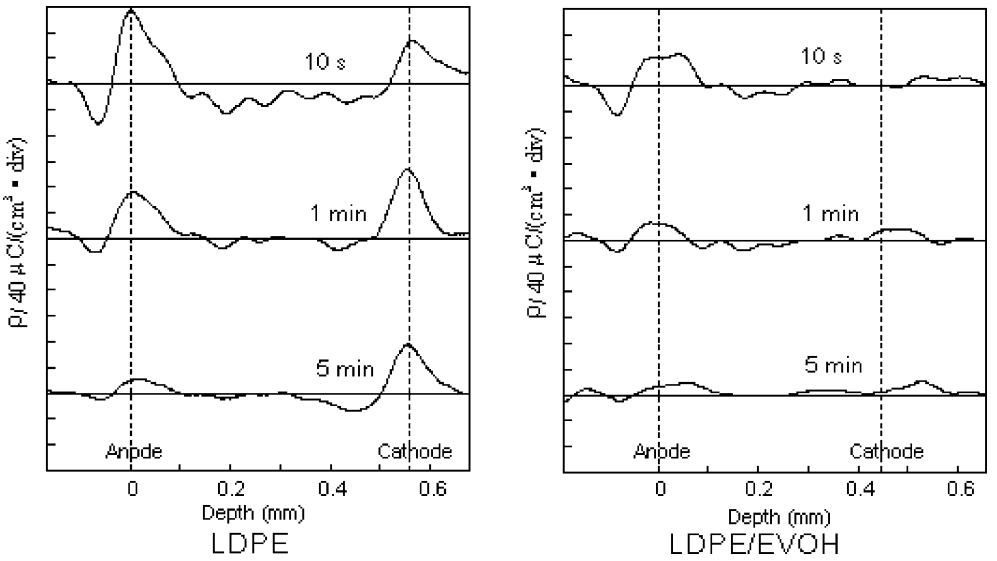

Fig. 3. Charge distributions after short circuit of LDPE and LDPE/EVOH.

(discharging) for 10 s, 1 and 5 min. Under DC voltages, it can be seen from Fig. 2 that the space charges in both samples are mainly hetero-charges. Most prominent negative space charges were observed near the anode. As the applied field intensity increases, the negative space charges near the anode increase remarkably. It is known that the hetero-charge in LDPE originates from migration, polarization, ionization, and orientation of low-molecular-mass species such as impurities, initiator residue, and additives. However, the density of space charges in LDPE/EVOH during charging is extremely small when compared to pure LDPE. From Fig. 3, it is also interesting to note that the discharge rate of LDPE/EVOH was much faster than that of LDPE. Within as short as 10 s, there were only few charges left in LDPE/EVOH. The remaining negative charge near the cathode after discharge is normally considered to be the result of the electrons injected from cathode and subsequently trapped in the samples during voltage application.

3.2. Morphology of LDPE/EVOH

The PEA measurement indicated that the space charges were decreased and the field distribution improved in LDPE by blending with 5 wt.% of EVOH. If LDPE/EVOH blend had co-continuous morphology, the space charge accumulated in the sample would easily dissipate through more conductive EVOH phase at discharge. However, the SEM observation shows that EVOH domain is surrounded by more resistive polyethylene matrix. Fig. 4(b) and (c) are the SEM pictures of the LDPE/EVOH blend, where the holes were EVOH domains removed by etching with nitric acid. LDPE and EVOH are completely incompatible due to the polarity of EVOH. From Fig. 4(c) the sharp interfaces between EVOH domain and LDPE matrix can be seen. It has been known that domain interfaces in immiscible polymer blends can act as trapping sites for homo-charges injected during the voltage application [20]. Therefore, the decrease of space charges in the LDPE/EVOH blend during the voltage application can be partially attributed to the domain interfaces, which trapped the homo-charge and resulted in an apparent decrease of hetero-charge.

On the other hand, upon removing voltage the charges will dissipate and return to the electrodes where they come from, if there are hopping sites through which charges can migrate. Accordingly, after discharge the decrease of space charges in the LDPE/EVOH blend should be related to the charge mobility in LDPE matrix. Because the LDPE component did not change chemically during blending, it is expected that the change of charge mobility is relative to the crystalline structure of LDPE matrix. Fig. 4(a) shows the crystalline spherulites in the LDPE sample, where the amorphous region between spherulites was partly etched by nitric acid and globular contour in diameter of $\sim$4 μm can be found. After blending the spherulites in the LDPE matrix became less distinct (see Fig. 4(c)), which size will be given from SALS measurements.

3.3. Crystalline form of LDPE matrix in the LDPE/EVOH

WAXD curves for the LDPE and LDPE/EVOH samples are shown in Fig. 5. Both samples have three

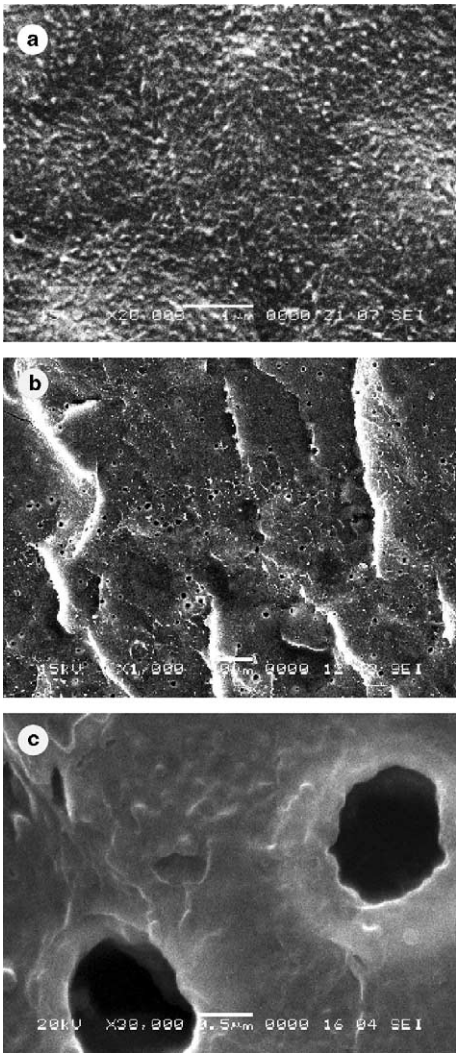

Fig. 4. SEM pictures of (a) LDPE (b) LDPE/EVOH and (c) LDPE/EVOH.

main crystalline diffraction peaks at 2θ of 21.4°, 23.7° and 36.1°, corresponding to the 110, 200, 020 lattice planes of the orthorhombic crystalline form of polyethylene. The amorphous scattering centered at 2θ of 19.8°. The refractions of monoclinic and triclinic forms were not found at the X-ray diffractogram. These results show that blending with 5 wt.% of EVOH did not change the crystalline form of LDPE. However, the inter-planar distance of the LDPE/EVOH was a little higher than that of the LDPE (see Table 2), which means that the order of macromolecules arrangement in crystalline lattices of polyethylene was slightly affected by blending with EVOH.

3.4. Size of spherulites of LDPE matrix in the LDPE/EVOH

A light scattering method was devoted to investigate crystalline superstructures in polymer films. The theories of spherulitic scattering were developed based upon the model of a homogeneous anisotropic sphere embedded in an isotropic medium. This approach successfully described the principal features of most experimental patterns. The H_V scattering gives the familiar four-leaf-clover-type pattern with its maximum intensity at the position angle (μ) of 45° and at a particular scattering angle (θ) which is inversely related to the size of spherulite [21], and the perfection of the spherulite lowers as the four-leaf-clover-type pattern diffuses. The relation between measured scattering vector at maximum scattering intensity (q_m) and spherulite size (R_S) can be written as the equation given below. So the size of spherulite can be roughly evaluated.

$$q_m R_S = 4.0 \tag{1}$$

where the scattering vector has the following form,

$$q = \frac{4\pi}{\lambda} \sin\frac{\theta}{2} \tag{2}$$

The SALS patterns and profiles of LDPE and LDPE/EVOH samples are shown in Figs. 6 and 7, respectively. The profiles of SALS are obtained from the scattering intensity ($\boldsymbol{I}$) against the scattering vector (q) at a certain position angle $\mu = 45°$. The SALS patterns for both samples are four-leaf-clover-type (see Fig. 6). Therefore, the crystalline morphologies of both samples appear to be spherulite. However, the major difference between them is the appearance of the contour of four-leaf-clover pattern. LDPE sample has a clear contour while the LDPE/EVOH sample has the diffused scattering pattern. The scattering curve for LDPE passes through a maximum at q of 1.6 μm^{-1} while the maximum for the LDPE/EVOH is at q of 2.6 μm^{-1} with larger half-width. The spherulite radius estimated from Eq. (1) is 2.5 and 1.5 μm for LDPE and LDPE/EVOH, respectively. These results indicate that the spherulites of LDPE become smaller and imperfect after blending with EVOH, which is consistent with results from SEM observation.

The decrease of spherulites size can be explained by the nucleation of crystallization of LDPE on the surface of EVOH domains. DSC analysis usually can be used to investigate the crystallization behavior of semi-crystalline polymers. Fig. 8 shows the corresponding DSC curves at the cooling rate of 10 °C/min. It is shown that crystallization of LDPE/EVOH started at higher temperature than that of virgin LDPE. In order to compare the crystallization rates of the two samples, the half-time $t_{1/2}$ was measured using depolarization method. The plot of $1/t_{1/2}$, which is proportional to the crystallization

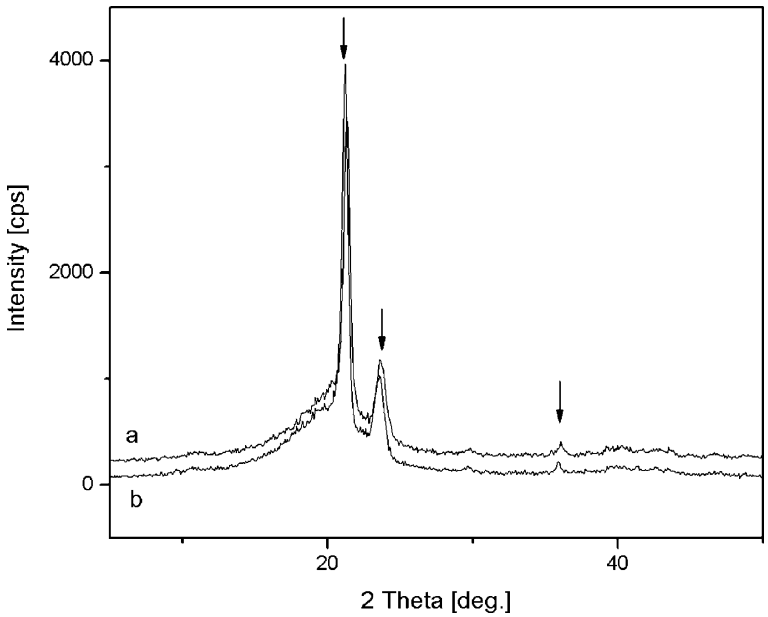

Fig. 5. WAXD diffractograms of (a) LDPE/EVOH and (b) LDPE.

Table 2
d-Spacing of crystal planes from WAXD analysis of LDPE and LDPE/EVOH

Sample	Crystal plane			
	110	200	020	210
LDPE	4.1487	3.7511	2.4833	2.9898
LDPE/EVOH	4.1603	3.7542	2.4860	3.0055

speed, versus temperature was given in Fig. 9. It can be seen that the crystallization rate of the LDPE/EVOH is much higher than that of the LDPE. These results implied that the EVOH in LDPE might play a role of nucleating agent for the crystallization of LDPE resulting in smaller spherulites.

In this study, non-isothermal crystallization was also conducted to determine the Avrami exponent n according to the method of Ozawa plots [15]. The measured Avrami exponent for LDPE is 1.73, which agrees well with the literature data ($n = 1.72$) [21]. The measured value of Avrami exponent for LDPE/EVOH is 1.36, which is appreciably lower than that for LDPE. The value of Avrami exponent may be composed of two parts: the contribution of the nucleation and the contribution of growth. The observed difference of the Avrami exponent may be essentially attributed to the nucleation. The Avrami exponent is close to 1 for the LDPE/EVOH and 2 for the LDPE. The integral value of LDPE/EVOH implies that it primarily forms one-dimensional crystallites from heterogeneous nucleation.

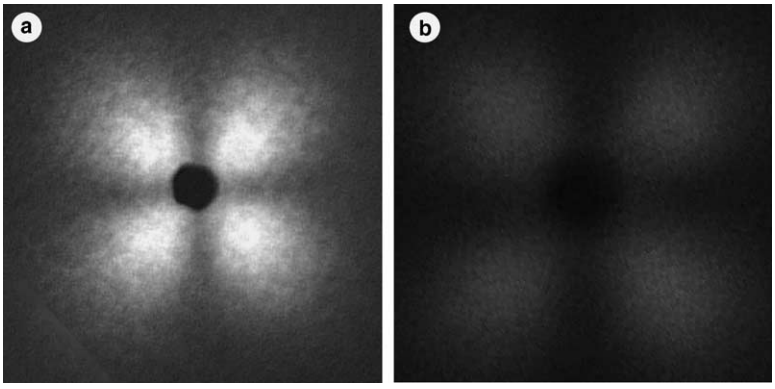

Fig. 6. Hv patterns of SALS: (a) LDPE and (b) LDPE/EVOH.

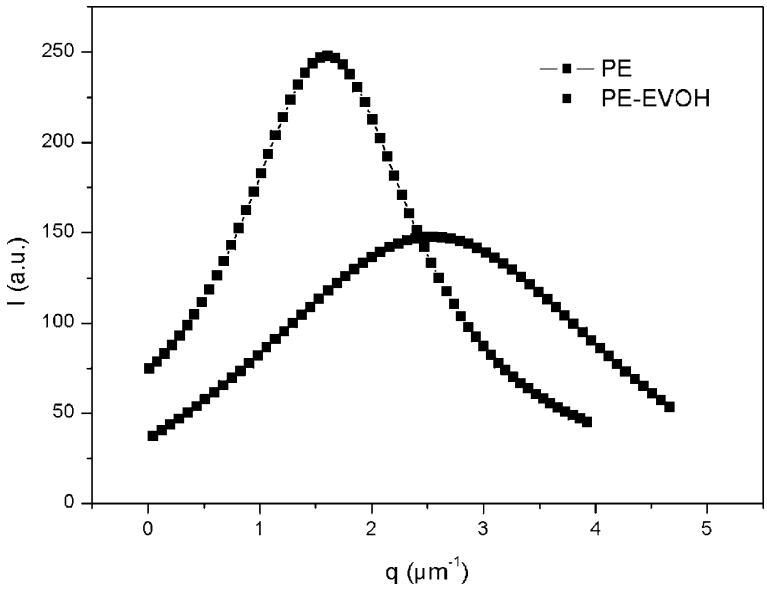

Fig. 7. SALS profiles of LDPE and LDPE/EVOH.

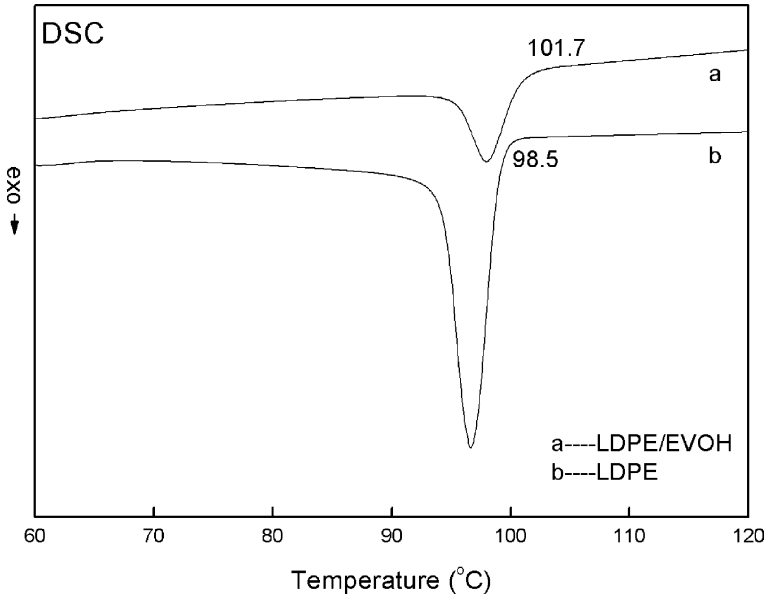

Fig. 8. DSC thermograms of non-isothermal crystallization for LDPE and LDPE/EVOH at the cooling rate of 10 °C/min.

In Table 3 the data of crystallinity from DSC at cooling rate of 10 °C/min are also listed. The LDPE/EVOH sample exhibits lower crystallinity. This is because the crystallization of polyethylene was influenced by the interfaces of the EVOH domains.

It is well known that during crystallization the "impurities" in polymer are usually expelled out and localized at the boundaries of spherulites, at the amorphous regions between crystalline lamellae, and at the defects of crystalline regions. In the case of polymers, "impurity" is a broad term covering weak polar molecules, initiator residues, macromolecular end segments, metal ions, and so forth. The regions of spherulites boundaries provided the path of migration for charge carriers. However, when perfect big spherulites are formed, the boundaries of spherulites will become the trapping sites blocking up the transportation of space charges because of its discontinuity or weak connection.

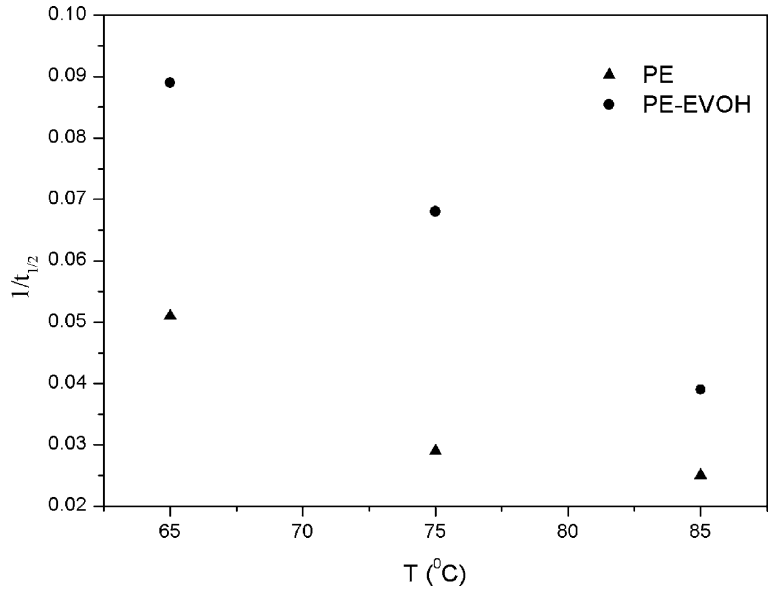

Fig. 9. $1/t_{1/2}$ versus temperature for LDPE and LDPE/EVOH.

Table 3
Crystallinity and Avrami exponent of LDPE and LDPE/EVOH

	LDPE	LDPE/EVOH
Avrami exponent, n	1.73	1.36
Crystallinity from DSC (%)	42.0	38.4

It has been reported that the conductivity of polymer is correlated to the spherulites size [22]. Vella and Toureille found that the space charge distribution in polyethylene film corresponded with the distribution of spherulites size, and attributed this phenomenon to higher conductivity in the outer region consisting of small spherulites and lower conductivity in the center having big spherulites [11]. It was also found in our previous paper [23] that small and imperfect spherulites may result in uniform distribution of space charge in DC field. In this study, the domain surface of EVOH, acting as a nucleating agent for LDPE, reduces the size and perfection of spherulites of LDPE. The decrease of the amount of homo-charges after discharging may be attributed to the smaller size of spherulites that result in the formation of dense and fine boundaries of spherulites, through which the charge can migrate. Therefore, the accumulated space charges will dissipate and return more easily to the electrodes where they came from.

4. Conclusions

The PEA measurements indicate that the amount of space charges of LDPE in DC field can be largely reduced by blending with 5 wt.% EVOH. The SEM observation shows that EVOH domains dispersed in the matrix of LDPE. The decrease of space charges in the blend during the voltage application can be partially attributed to the sharp domain interfaces that traps the homo-charges and results in an apparent decrease of hetero-charges. The results of DSC measurement and SALS analysis imply that blending with EVOH diminishes the spherulites size of LDPE. The improvement of space charge distribution after discharging is probably attributed to the smaller size of spherulites.

Acknowledgements

This work is subsidized by the Special Funds for Major State Basic Research Projects (G1999064800).

References

[1] Keiichi K, Goro S, Masayuki I. Jpn J Appl Phys 1980; 19:389.
[2] Suh KS, Hwang SJ, Lee C. IEEE Trans Dielect Electr Insul 1997;4:58.
[3] Suh KS, Koo JH, Lee SH, Park JK, Takada T. IEEE Trans Dielect Electr Insul 1996;3:153.
[4] Suh KS, Kim JY, Lee CR, Takada T. IEEE Trans Dielect Electr Insul 1996;3:201.
[5] Suh KS, Lee CR. IEEE Trans Dielect Electr Insul 1997; 4:681.
[6] See A, Dissado LA, Fothergill JC. IEEE Trans Dielect Electr Insul 2001;8:859.

[7] Fanjeau O, Mary D, Malec D. J Phys D: Appl Phys 2000; 33:61.
[8] Meunier M, Crine JP. IEEE Annu Rep, Conf Electr Insul Diel Phenom, 1985. p. 377–81.
[9] Crine JP. IEEE Trans Dielect Electr Insul 2002;9:697.
[10] Fan ZH, Yoshimura N. IEEE Trans Dielect Electr Insul 1996;3:849.
[11] Khalil MS, Cherifi A, Toureille A, Reboul JP. IEEE Trans Dielect Electr Insul 1996;3:743.
[12] Li X, Cao Y, Du QG, Tu DM. J Appl Polym Sci 2001; 82:611.
[13] Ieda M. IEEE Trans Dielect Electr Insul 1984;19:162.
[14] Lopez LC, Wilkes GL. Polymer 1989;29:106.
[15] Ozawa T. Polymer 1971;12:150.
[16] Kozlowski W. J Polym Sci Part C 1970;38:47.
[17] Eder M, Wlochowicz A. Colloid Polym Sci 1983;261:621.
[18] Wunderlich B, Cormier CM. J Polym Sci Part A-2 1967; 5:987.
[19] Liu B, Du QG, Yang YL. J Membr Sci 2000;180:81.
[20] Suh KS, Lee HJ. IEEE Trans Dielect Electr Insul 1995;2:460.
[21] Gupta AK, Rana SK, Deopura BL. J Appl Polym Sci 1994;51:231.
[22] Ku CC, Liepins R. In: Electrical properties of polymer chemical principles. New York: Hanser Publisher; 1987. p. 328.
[23] Li X, Du QG, Kang J, Tu DM. J Polym Sci Polym Phys 2002;40:365.